

The Proportionality between Charge Acceleration and Radiation from a Generic Wire Object

Edmund Miller*

Abstract—The Lienard-Wichert potentials show that radiation is caused by charge acceleration. The question arises about where charge acceleration occurs on the most basic of antennas, a center-fed, perfectly conducting dipole, for which there are two obvious causes. One is the feedpoint exciting voltage that sets into motion an outward-propagating charge and current wave at light speed c in the medium. A second is at the dipole ends where the outgoing wave is totally reflected producing a change in charge speed of $2c$. In addition there is the decreasing amplitude of the propagating wave with distance due to its partial reflection along the wire. That reflected charge also undergoes a speed change of $2c$. This is the reason why the decay of current flowing along a straight wire antenna has been attributed as being due to radiation. Radiation caused by these and other kinds of charge acceleration due to resistive loads, right-angle bends, and radius steps are investigated. These phenomena are examined primarily in the time-domain where they are more observably separable in time and space than in the frequency domain. The current and charge induced on an impulsively excited wire antenna and its broadside radiated E-field are computed using a time-domain, integral-equation model. The computed results are used to derive a numerical relationship between the amount of accelerated charge and its radiated field. This relationship is denoted as an Acceleration Factor (AF) that is obtained for various charge-accelerating features of a generic wire object are normalized to that of the exciting source for comparison with their respect speed changes.

1. INTRODUCTION

The Lienard-Wichert potentials show that charge acceleration causes radiation [1]. Thus, in order to develop a quantitative understanding of radiation from a perfect-electric conductor (PEC) excited as an antenna, it's necessary to determine where and how much charge acceleration occurs on it. It is well accepted that a dipole antenna radiates from its feedpoint and ends, but there is some disagreement about whether it radiates elsewhere [2, 3]. Numerous authors [4–17] associate the current decay down a long-wire antenna as being due to radiation. This seems plausible since the current decay means that the corresponding longitudinal Poynting's vector then carries less power or energy with increasing distance [17]. But if current decay causes radiation this means that charge acceleration is somehow involved. Charge acceleration occurs because some charge reflects in a direction opposite to that of the propagating wave, similar to what happens at the end of the wire, an observation made by only one of the references above [16]. It is clear that wherever charge reflection occurs on an antenna radiation results. Feedpoint and various reflection-caused radiation mechanisms are explored quantitatively in the following.

Received 20 February 2018, Accepted 29 April 2018, Scheduled 11 May 2018

* Corresponding author: Edmund Miller (e.miller@ieee.org).

The author is with the Los Alamos National Laboratory (Retired), 597 Rustic Ranch Lane, Lincoln, CA 95648, USA.

2. CHARGE REFLECTION AND RADIATION

Detailed attention in this article is primarily focused on a PEC straight wire for simplicity. However, it is illuminating to consider conceptually a more general wire object as sketched in Figure 1. The radiation due to charge acceleration associated with each highlighted feature denoted by alphabetical letter is briefly listed below.

- (i) A spatially varying wave impedance that produces charge reflection along a straight section of wire, or what is called here “propagation radiation”.
- (ii) Any electric field applied to the object in Figure 1, whether from some external excitation such as an incident plane wave or from a localized source such as the feedpoint of an antenna that will cause a current to flow in response. Setting charge into motion produces accompanying acceleration that causes radiation.
- (iii) Charge reflection at an open end of a wire is another cause of radiation. It’s worth noting that reflection produces a charge speed change of $2c$ whereas a source field as at B causes a change of c .
- (iv) Charge reflection from a lumped impedance.
- (v) A directional change in charge velocity at a sharp bend or smoother curvature produces charge reflection and charge acceleration that causes radiation. (Velocity is used here when a directional effect occurs, but when only straight-line motion is involved the term used is speed).
- (vi) Charge reflection at a change in wire radius.

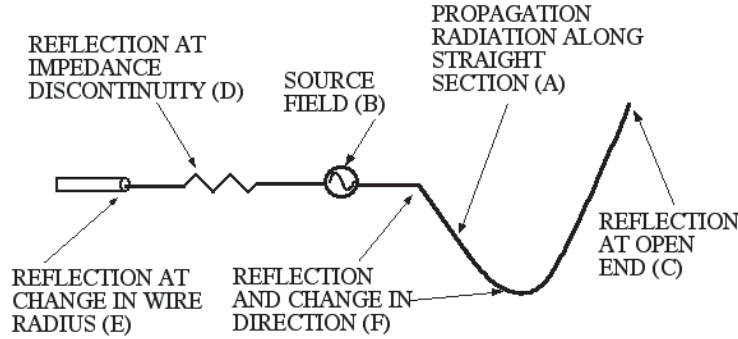


Figure 1. A generic wire object exhibiting various features that cause radiation.

That charge acceleration causing radiation can be demonstrated graphically using the E-field kink model of radiation [18]. This is shown analytically by the Lienard-Wiechert potentials [1] from which the radiated component of the electric field due to a charge q can be written as

$$\mathbf{E} = \frac{q}{4\pi\epsilon_0 c^2 s^3} \left\{ \mathbf{r} \times \left[\left(\mathbf{r} - \frac{r\mathbf{u}}{c} \right) \times \frac{d\mathbf{u}}{dt'} \right] \right\} = qK \left\{ \mathbf{r} \times \left[\left(\mathbf{r} - \frac{r\mathbf{u}}{c} \right) \times \mathbf{a} \right] \right\} \quad (1a)$$

$$\text{where } s = r - (\mathbf{u} \cdot \mathbf{r})/c. \quad (1b)$$

Equation (1) yields the electric field \mathbf{E} of a charge q moving with velocity \mathbf{u} and acceleration \mathbf{a} along a prescribed path in space. There is no radiation unless \mathbf{a} is nonzero. Applications of Equation (1) include accelerator design and analysis of electron lasers. Charge acceleration (1) is not explicitly included in a computer model such as TWTD (Thin-Wire Time Domain) [19] that was developed for modeling a PEC. But the effect of acceleration can be derived from the results TWTD provides as will be shown below. It is the primary goal of the following discussion to develop a quantitative relationship between \mathbf{E} and q for the various kinds radiation that can occur on the type of PEC object in Figure 1. This is done by conducting computer experiments using two well-validated computer codes, TWTD for time-domain results and NEC (Numerical Electromagnetics Code) [20] for frequency-domain results.

Radiation due to charge acceleration is caused by a source field, and several kinds of charge reflection are evaluated in the following. The goal is to develop from computed TWTD results a quantitative

estimate of the relationship between the accelerated charge and $E_{||}$, the broadside, electric field parallel to a straight section of a wire that it radiates. The proportionality between the numerically computed charge and radiated electric field values from TWTD is expressed here as an Acceleration Factor (AF). Thus, the absolute value of $|E_{||}|$ can be written as

$$|E_{||}| = AF \times |Qc|, \tag{2a}$$

$$\text{so that } AF = |E_{||}|/|Qc| \tag{2b}$$

with Q the total accelerated charge density on the wire associated with a particular $|E_{||}|$. Absolute values are used here for Qc and $E_{||}$ since charge pulses of opposite signs simultaneously accelerated in opposite directions can produce additive fields of either sign. For the case of source, propagation and end-reflection radiation (A, B and C of Figure 1) the pulse shapes from TWTD are used from (2b) to illustrate the temporal correlation between $E_{||}$ and Qc . Otherwise, the numerical AF values are obtained using the corresponding peak values of these quantities to show the effect of some parameter variation such as length, radius or resistance loads. The absolute AF values obtained from the various cases investigated are not themselves of primary interest here. It is rather to establish to what extent $E_{||}$ and Qc are proportional in time or to a particular parameter. Also of interest are their values relative to that of an exciting source. This is because the source causes a change of c in the charge speed while any reflection results in a $2c$ speed change, a phenomenon that is illustrated further below.

Unless stated otherwise, a wire radius of 10^{-3} m is used throughout together with a segment length, Δx , in the frequency domain of 0.01 wavelengths and in the time domain of 0.01 m, with the time step $\Delta t = \Delta x/c$. Some other materials related to the discussion that follows can be found in References [21] and [22]. The excitation is a 1-V peak Gaussian pulse for all time-domain results presented in the following.

3. CURRENT DECAY AND PROPAGATION RADIATION IN THE FREQUENCY DOMAIN

The current on an infinite PEC wire antenna varies with distance z from its feedpoint as [8]

$$I_{\infty}(z) = \frac{ie^{ikz}}{\eta_o} \log \left\{ \frac{2\pi i}{2C_w + \log \left(kz + [(kz)^2 + e^{-z\gamma}] + \gamma + i\frac{3}{2}\pi \right)} \right\} \tag{3a}$$

$$\text{where } C_w = \log(1/ka) - \gamma \tag{3b}$$

$$\text{and } \gamma = 0.57721566 \text{ (Euler's constant)} \tag{3c}$$

with k the wavenumber of free space and a the wire radius.

The envelope of maximum current magnitude from Eq. (3) is plotted in Figure 2 normalized to its value at 0.16 wavelengths from the feedpoint for $ka = 0.01$. It decays monotonically with increasing distance from the feedpoint due to propagation radiation (A in Figure 1). By contrast, the outward-flowing current on an infinite biconical antenna does not decay with distance, as given by [23]

$$I(r) = I_o e^{-ikr}, \tag{4}$$

with I_o the input current. Because the wave admittance of a conical structure is independent of r there is no reflected current and thus no current decay. Consequently, radiation from the infinite bicone originates only from its feedpoint where the tips of the two bicones are joined.

The on-surface longitudinal Poynting vector of a 10-wavelength, center-fed dipole consequently also decays with distance as shown in Figure 3 [17]. This is obtained from the dipole's radial electric field (charge density) and azimuthal magnetic field (current density) using NEC. The power flow is somewhat oscillatory while declining monotonically with increasing distance from the dipole feedpoint. The significance of the current reflection and consequent decrease in power or energy flow is explored next.

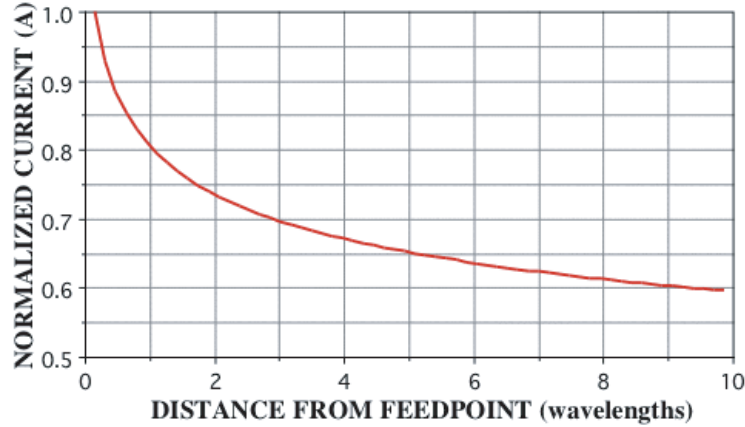


Figure 2. The envelope of maximum current magnitude from Shen et al. [8].

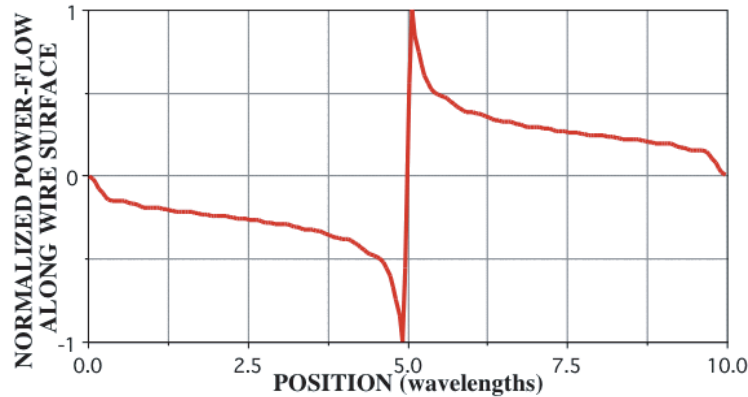


Figure 3. The on-surface, longitudinal Poynting vector obtained from NEC for a center-fed, 10-wavelength dipole [17].

4. A PREVIEW OF RADIATION AND CURRENT DECAY FOR A STRAIGHT WIRE

Before developing AF estimates for the various cases to be considered, it is instructive to examine some initial results for long straight wires. The current I and charge-density Q times light speed c are shown at several time steps in Figure 4 on a dipole 599 segments long excited at its center by a 1-V Gaussian pulse. It is clear that the positive I and Qc -pulses are numerically equal on the right-hand side of the dipole (i.e., $Qc = I$) but of opposite sign on the left-half side. This is because a positive charge moving to the right produces a positive current, as also does a negative charge moving in the opposite direction to the left. Their numerical equality implies that the current and charge carry the same amount of energy, an effect that is demonstrated explicitly in Section 12. It's also clear that their amplitudes decay monotonically with increasing distance from the feedpoint. As for the frequency domain, this decay exhibits the effect of partial charge reflection. This reflection produces the smaller negative current components trailing the positive current pulses on Figure 4.

Observe that on the impulsively excited, center-fed dipole used to obtain the results of Figure 4, the partial reflection of the rightward-moving positive-charge pulse and the partial reflection of the leftward-moving negative-charge pulse cause acceleration of both reflected pulses. This acceleration produces kinks in their electric field lines in accordance with the E-field kink model [18], to produce $1/R$ outward-propagating electric fields as kinks in their respective field lines. Since the charges are of opposite sign and accelerated in opposite directions their radiation fields have the same polarity and

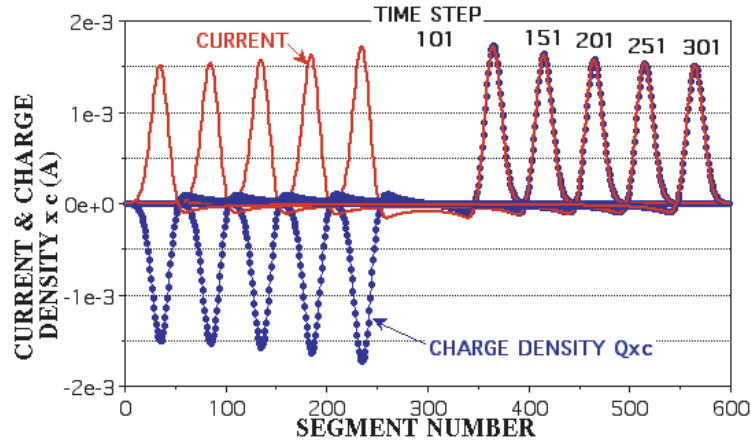


Figure 4. Charge density Q times light-speed c and the current I for a 599-segment wire excited at its center by a Gaussian voltage pulse at several time steps.

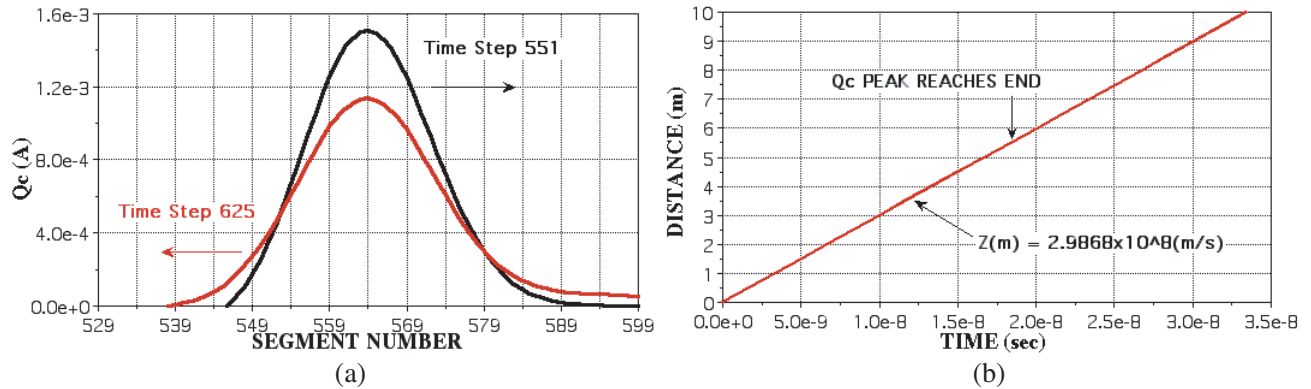


Figure 5. Incident (black) and reflected (red) (a) Qc pulses near the end and (b) a distance-time plot for Qc pulses on a 599-segment straight wire.

are thus additive.

The Qc and current pulses in Figure 4 show somewhat indirectly that they propagate at the speed of light. The plot in Figure 5 shows more explicitly that this is the case for excitation of the 599-segment wire at segment 49 near its left end. Plotted there at time steps 551 and 625 are the initially rightward-propagating Qc pulse and its leftward-propagating reflection from the wire end in (a). The total distance traveled by the incident and reflected Qc pulses is plotted as a function of time in (b). A best-fit straight line to this plot reveals a propagation speed of 2.9868×10^8 m/sec, a value that is 99.56% of the specified light speed of 3×10^8 in TWTD. Considering the approximations inherent in a discretized model, this small difference seems reasonable. The arrow indicates the time at which the Qc pulse reaches the wire’s end. Even though there is a slight slowing in the pulse speed during end reflection (see Section 12) it is not enough to be discernable in Figure 5(b).

The radiated, broadside E-field for the time between turning on of a center, impulsive excitation and the first end reflection of the outgoing current and charge pulses for various wire lengths is plotted in Figure 6. Observe that the first E-field pulse occurs as the exciting source initially sets current and charge into motion. The second pulse is produced by the outward-propagating current and charge pulses, such as shown in Figure 4, reflecting from the ends of the dipole. Connecting these two radiation pulses is a continuous, decreasing radiation field due to reflection of the outward-propagating charge pulses, denoted here as propagation radiation.

Note that propagation radiation from a partially reflected charge pulse propagating along the wire

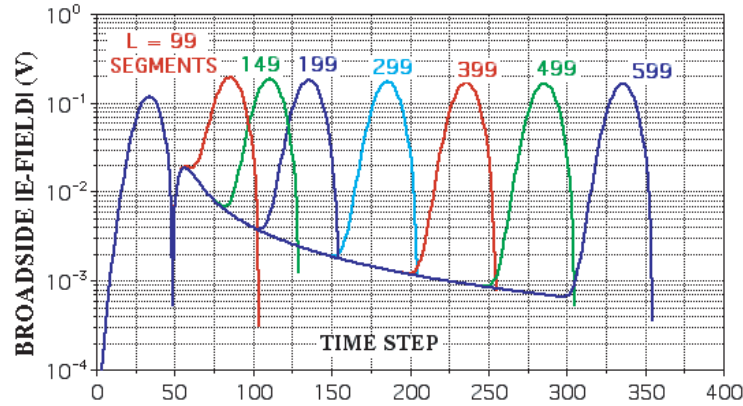


Figure 6. Magnitudes of the broadside radiated E-fields versus time step for impulsively excited, center-fed straight wires of various lengths.

is qualitatively the same as the end-reflection radiation that occurs when the entire pulse reflects from the open end of the wire. In both cases the change in speed of the reflected charge is $2c$. However, observe that the propagation radiation that results is less than end-reflection radiation because less charge is reflected in the propagating phase. Also, while their total speed changes are the same, their associated accelerations are not necessarily so. This is possible if the time over which the speed changes differ because their respective reflection processes differ, something that is discussed in connection with end reflection in Section 12. That the source-accelerated charge undergoes a speed change of only c while the end-reflection change is $2c$ accounts for their respective radiated peak fields of the latter in Figure 6 being almost twice as much.

5. COMPARING CURRENT DECAY ON A LONG WIRE AND CIRCULAR LOOP

Current decay over a greater distance and time duration is shown in Figure 7(a). A sequence of current pulses at 100 time-step intervals is plotted for a straight wire 1199 segments in length excited near its left end at segment 49 by a 1-V Gaussian voltage pulse. Also plotted in Figure 7(a) for comparison are equivalent results for a circular loop 1199 segments in circumference. For clarity both plots include only the positive current pulses propagating away from the feedpoint to the right for the dipole and clockwise for the loop. The speed of the loop-current peaks is $\sim 3.0168 \times 10^8$, or somewhat faster than that on the straight wire, as can be seen in Figure 7(a). This is apparently because the straight-line distance between two points on an arc is less than that on a straight wire of the same length so that the interaction fields have a shorter distance to travel. This effect also accounts for the gradual spreading out of the leading edge of the loop current.

The normalized envelopes of the peaks in the current-pulse amplitudes obtained from the results of Figure 7(a) are presented in Figure 7(b). Note the similarity of the time-domain dipole current decay with the frequency-domain plot of Figure 2 above. Current-pulse decay on the circular loop exceeds that on the straight wire because the loop curvature produces increased charge reflection. Subsequent attention is limited hereafter to the straight wire because its broadside far field is more easily related to its propagating current and charge due to the more straightforward time-delay differences from various parts of the straight wire.

6. SOURCE-REGION RADIATION

The broadside E-field magnitude caused by the feedpoint Qc pulse is plotted in Figure 8 where an acceleration factor AF_S of 29.4 is obtained, a result that is independent of wire length as demonstrated in Figure 6. This independence of wire length occurs so long as the time duration of the excitation is less than the propagation time along the wire. On the other hand the exciting-source radiation pulse

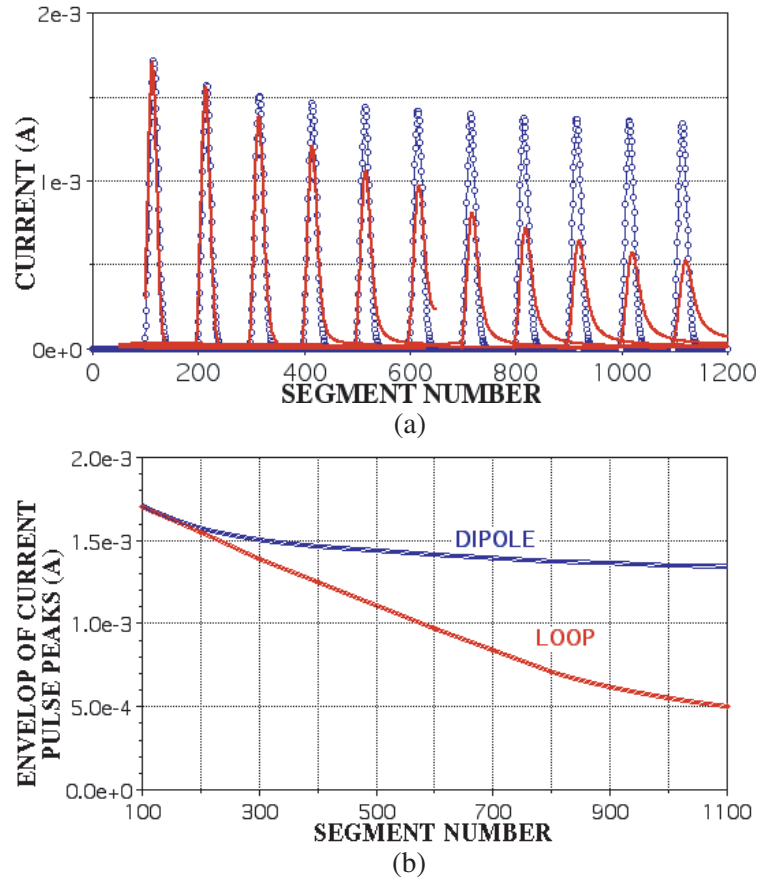


Figure 7. The rightward-propagating positive current pulses on a 1,199-segment straight wire (blue) and clockwise on a circular loop (red) at (a) intervals of 100 time steps excited by a Gaussian voltage pulse, (b) whose envelopes are plotted as a function of distance from segment 100.

is dependent on wire radius as demonstrated in Figure 9. The magnitude of the peak radiation E-field pulse for various wire radii is plotted as a function of the charge-pulse peak produced at the exciting source. The average source-acceleration factor for the variable-radius case, AF_{SR} , is 29.2. This result confirms the linear relationship expected from the Lienard-Wiechert potentials that the radiated field is proportional to the charge.

7. PROPAGATION RADIATION

Reflection of a propagating charge pulse in frequency-domain results is exhibited as a decay of the outward propagating current of Figure 2 above. In the time-domain results of Figures 4, 6 and 7 it is exhibited directly in the decreasing pulse amplitudes with distance and indirectly as a negative trailing component of the outward-propagating positive current pulses in Figure 4.

The reflection of the current and charge demonstrates that the wave impedance presented by the wire does not match that of the propagating pulses, as discussed in [9]. The integrated charge in the rightward-propagating Qc pulse is plotted as a function of time in Figure 10(a) for time steps T and $T + 1$. The difference between the two plots of Figure 10(a) is shown as the amount of charge reflected per time step in Figure 10(b). A comparison of the broadside propagation-radiation E-field with the reflected Qc charge of a 599-segment wire multiplied by an AF_P of 33.1 is plotted in Figure 11.

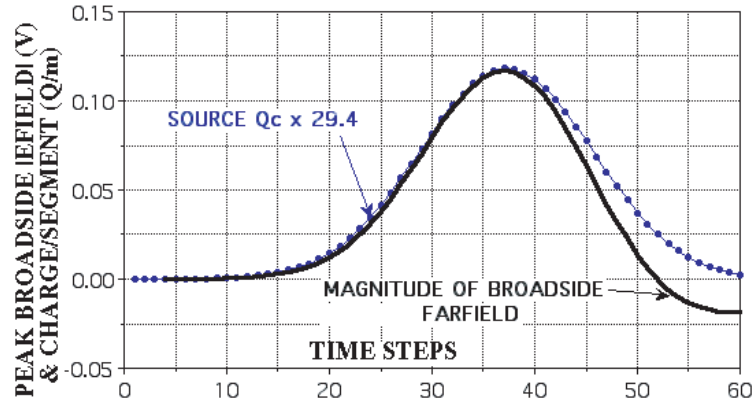


Figure 8. Time plots of the magnitudes of the broadside E-field and the source-induced charge of the 599-segment dipole as a function of time to exhibit their proportionality with the a source acceleration factor AF_S of 29.4.

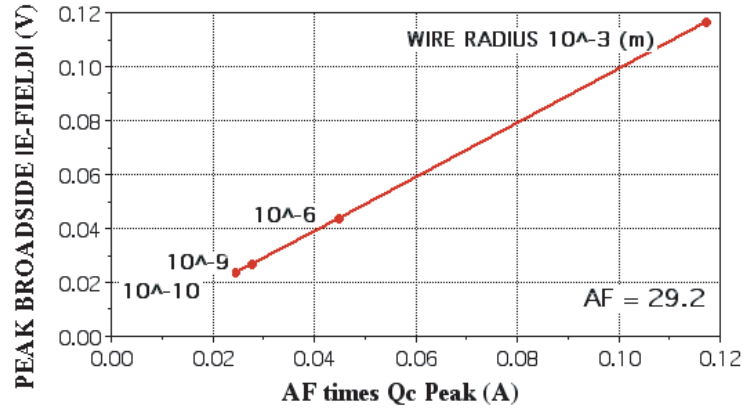


Figure 9. The magnitude of the peak broadside electric field due to the exciting-source charge as the dipole wire radius is varied over 7 orders of magnitude to exhibit their proportionality with an average acceleration factor AF_{SR} of 29.2.

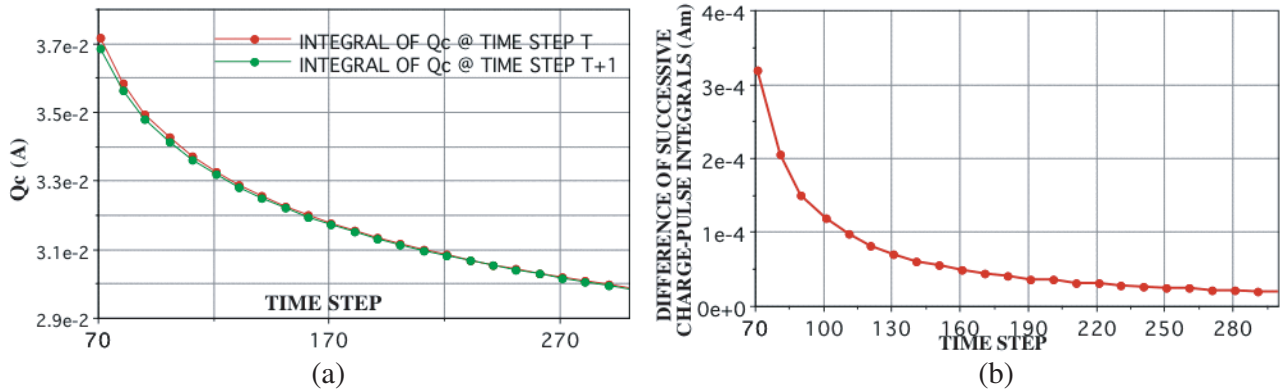


Figure 10. (a) The positive space integrals of Q_c at successive time steps on the right-hand half of the 599-segment dipole and (b) the difference between successive positive Q_c pulses on the right-hand half of the dipole in (a) as a function of time.

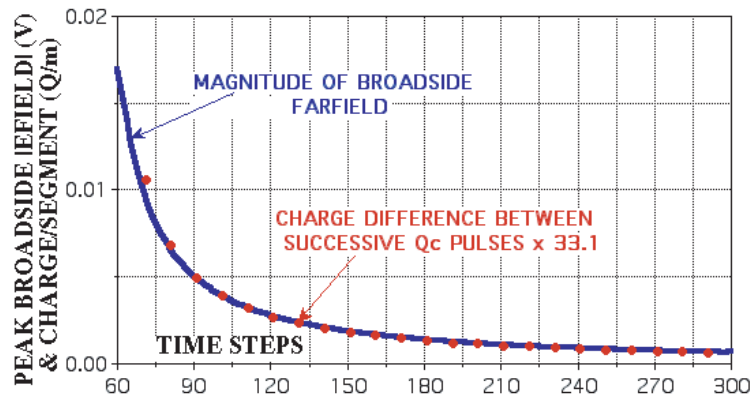


Figure 11. Time plots of the magnitude of the broadside E-field and the reflected charge on a 599-segment dipole as a function of time to exhibit their proportionality with an acceleration factor AF_P of 33.1.

8. REFLECTION RADIATION FROM THE END OF A WIRE

The reflection radiation from a wire end is plotted for a 599-segment wire as a function of time step in Figure 12 where the AF_E is 53.5. This is 1.83 times that of the average exciting-source radiation, AF_S of Figure 9. This ratio reflects the fact that the source-accelerated charge undergoes a speed change of c while the end-reflection charge experiences a speed change of $2c$. The fact that this ratio is not 2 apparently demonstrates that end-reflection acceleration is not quite as abrupt as the acceleration due to the exciting source. This point is further discussed in Section 12 in connection with the energy carried by the current and charge. The end-reflection radiation-field peak was shown to decrease with increasing dipole length in Figure 6, due to the decreasing amount of charge that reaches its end due to charge reflection along the wire. This is demonstrated quantitatively in Figure 13. The results for the propagation, source and end-reflection radiation are illustrated together in the combined plots of Figure 14.

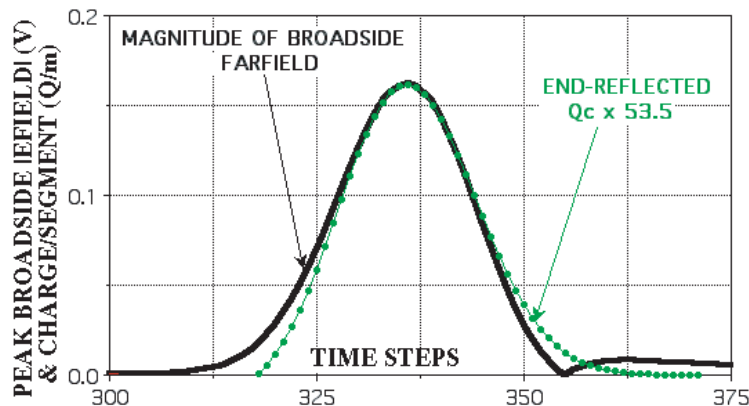


Figure 12. Time plots of the magnitude of the end-reflected E-field and the end-incident charge on a 599-segment dipole as a function of time to exhibit their proportionality with an acceleration factor AF_E of 53.5.

9. REFLECTION RADIATION FROM RESISTIVE LOADS

The magnitude of the peak broadside radiated E-field caused by charge reflection from a lumped, resistive load is presented in Figure 15 for a wire 199 segments long. A Gaussian voltage pulse is

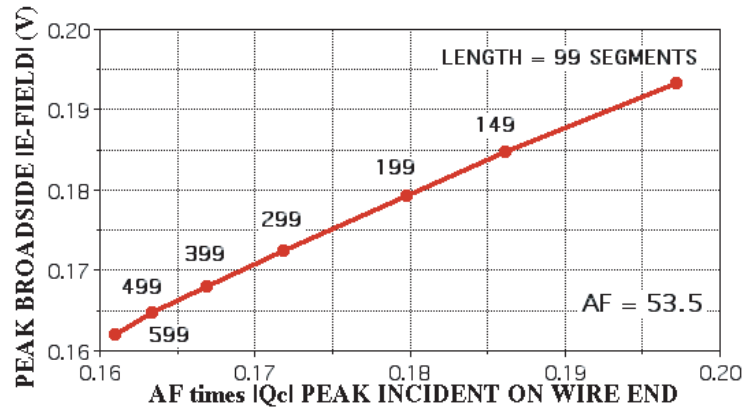


Figure 13. The decrease in the peak broadside electric field caused by a decreasing end-reflected Q_c pulse with the wire length a parameter.

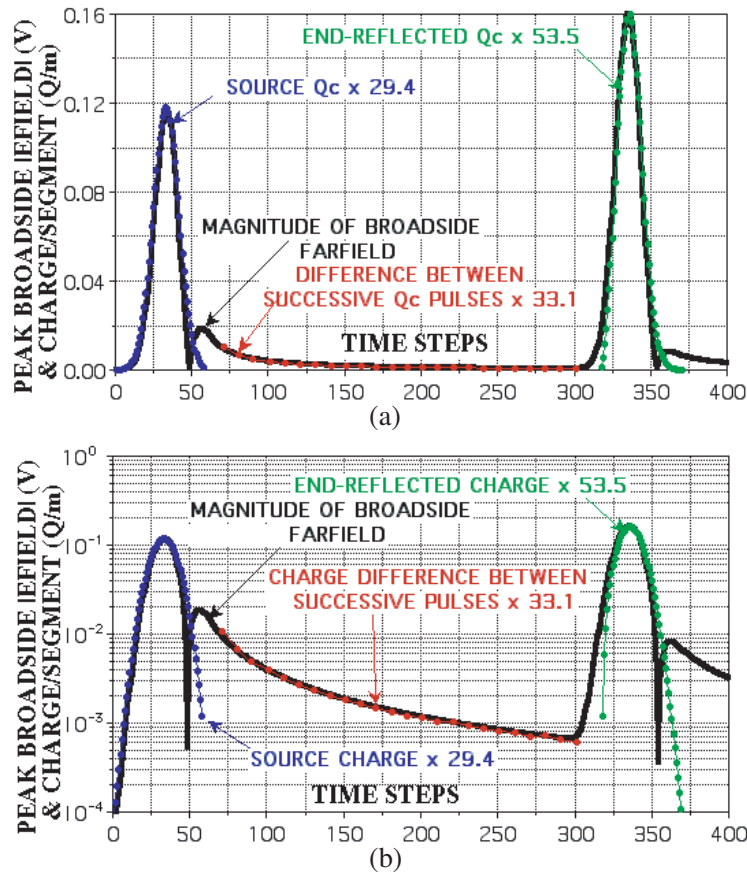


Figure 14. Combined plots of the propagation, source and end-reflected broadside E-field magnitudes and the respective time varying accelerated Q_c charge pulses that produce them on a (a) linear plot and (b) log plot.

applied at segment 75 with the load located at segment 100. As for the various similar plots above, the radiation field is proportional to the reflected charge with an average acceleration factor AF_R for this case of 34.1.

10. RADIATION FROM DIRECTIONAL REFLECTION AT A 90-DEG BEND

Reflection radiation caused by a 90-deg bend is plotted with the wire radius a parameter in Figure 16 for a 199-segment wire excited impulsively at segment 75 with a bend at segment 100. The acceleration factor, AF_B , is found to be 30.3. Only a 90-deg bend is examined here as this results in radiation from the bent portion of the wire being orthogonal to that from the other wire half. If the bend were different from 90-deg, identifying what part of the radiated E-field comes from the two halves of the wire would be less clear. The plot of Figure 16 continues the relationship established in the previous results that show an essentially linear proportionality between the peaks of the reflected Q_c and broadside radiated E-field pulses.

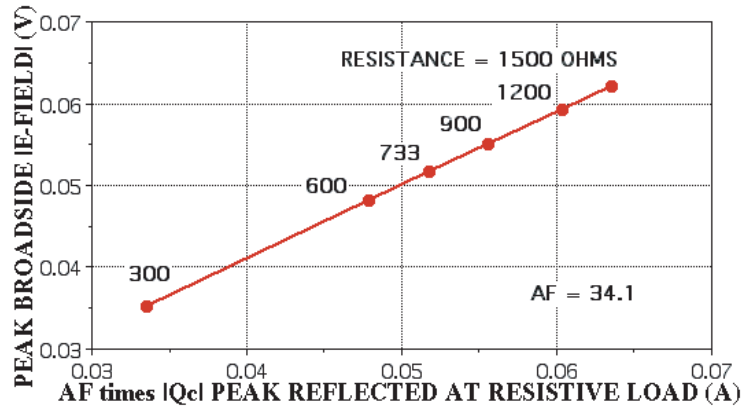


Figure 15. The peak broadside E-Fields caused by charge reflection from lumped, resistive loads of various values.

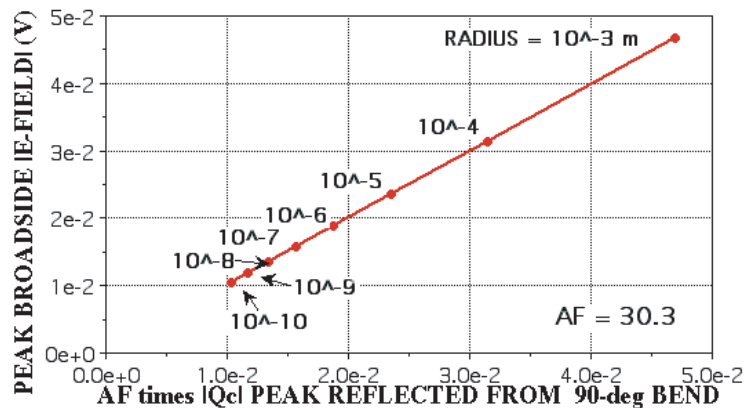


Figure 16. The peak magnitudes of the broadside E-field and the reflected Q_c pulse from a right-angle bend for an impulsively excited wire 199 segments long with wire radius a parameter.

11. REFLECTION RADIATION FROM A STEP IN THE WIRE RADIUS

The remaining example for a radiation feature from the generic object of Figure 1 is a step change in wire radius. But in contrast with previous results where the reflected Q_c pulses are clearly defined, this was not found to be the case for the step-radius wire. Instead, the step effect is more clearly demonstrated in a frequency-domain radiation pattern such as shown in Figure 17. The radiation pattern of a sinusoidal current filament (SCF) is plotted for comparison together with the patterns of two center-fed, 200-segment dipoles modeled using NEC. Each dipole is 10 wavelengths long with a

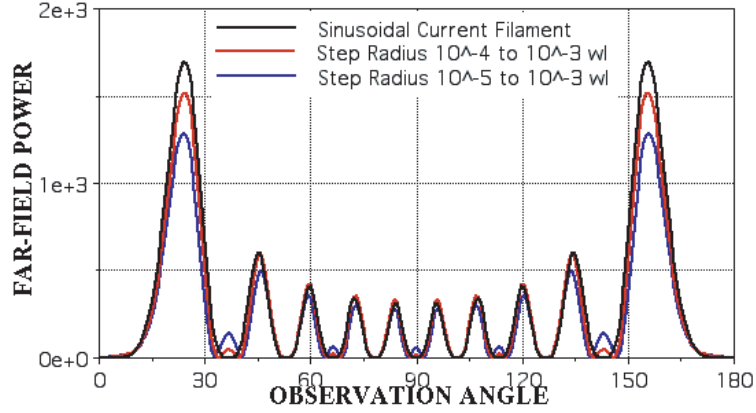


Figure 17. The radiation patterns for a 10-wavelength sinusoidal current filament and two NEC dipoles having radius steps at 1/4 and 3/4 of their lengths with each having a 1-A maximum current.

center section of 100 segments and a radius of 10^{-3} wavelengths. The end sections are 50 segments long each and have radii of 10^{-4} and 10^{-5} wavelengths respectively. The current magnitudes for each are 1-A.

The SCF and the step-dipole patterns in Figure 17 are similar with respect to their main lobes. The effect of the radius steps is to cause 5 smaller lobes to appear at two-lobe intervals between the larger lobes beginning at broadside, an effect that increases with an increasing in step radius. These results provide indirect evidence for the radiation caused by a step in the wire radius.

12. AN ENERGY MEASURE THAT DEMONSTRATES RADIATION LOSS

One way to evaluate the energy radiated by an impulsively excited object is to integrate the far fields over an enclosing sphere as a function of time, something that can be computationally expensive. An alternative demonstrated here is to instead integrate the boundary sources over the object at each time step of the numerical solution [24].

This is done here for a wire dipole impulsively excited at its center using

$$W_I(t) = \int_0^L I^2(x \cdot t) dx \quad (5a)$$

and

$$W_{Qc}(t) = c^2 \int_{-\frac{L}{2}+\Delta}^{\frac{L}{2}-\Delta} Q^2(x, t) dx + \frac{c^2}{3} \left[\int_{-\frac{L}{2}}^{-\frac{L}{2}+\Delta} Q^2(x, t) dx + \int_{\frac{L}{2}-\Delta}^{\frac{L}{2}} Q^2(x, t) dx \right] \quad (5b)$$

where $W_I(t)$ and $W_{Qc}(t)$ are the current (or magnetic) and charge (or electric) energy measures at time t and Δ is the segment length in the numerical model. The two terms in the bracketed portion of Equation (5b) account for the fact that the propagation speed of the charge pulse going to zero at the ends of the wire cannot happen instantaneously. This fact is approximated for by assuming that the squared speed falls linearly to zero over the last segment of the numerical model. The $c^2/3$ is an average that comes from

$$c_{ave}^2 = \frac{1}{\Delta} \int_0^{\Delta} \left[\frac{cx}{\Delta} \right]^2 dx = \frac{c^2 x^3}{3\Delta^3} \Big|_0^{\Delta} = \frac{c^2}{3}. \quad (6)$$

Observe that if the 1/3 is not used in Equation (5) the total energy no longer decreases monotonically, but rises at end reflection, a non-physical result. This result in Eq. (6) also offers some indication about how the acceleration term in the Lienard-Wiechert potentials might be influenced by the particular details of the radiation features discussed in connection with Figure 1.

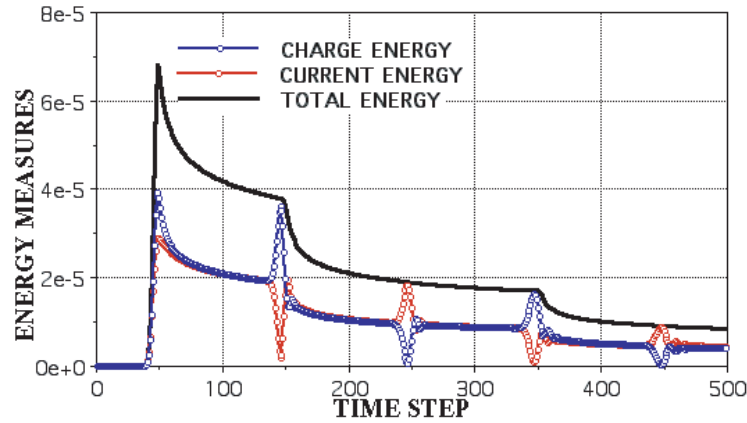


Figure 18. The current, charge and total energy measures as a function of time for an impulsively excited straight wire 199 segments long.

Results for these two quantities and their sum are presented for a center-fed dipole 199 segments long in Figure 18. After the startup transient, $W_I(t)$ and $W_{Qc}(t)$ are equal until the I and Qc pulses reach the end of the wire where $W_{Qc}(t)$ becomes predominant as the charge accumulates there and the current goes to zero. Upon reflection, their equality is reestablished until the oppositely propagating pulses meet at the wire center where $W_I(t)$ becomes predominant since the current is additive while the charge pulses cancel. After each end reflection, the total energy exhibits a marked decline due to the end-reflection radiation. This behavior continues periodically until the wire returns to charge neutrality. As a result, the total propagating energy decreases monotonically due to the effects of end-reflection and propagation radiation.

13. SUMMARY OF THE DERIVED ACCELERATION FACTORS

The various acceleration factors developed from the above results are summarized for reference in Table 1.

Table 1.

RADIATION TYPE	ACCELERATION FACTOR	NORMALIZED AF
Source: AF_S	29.4	1.0
Source: Variable Wire Radius: AF_{SR}	29.2	0.99
Right-Angle Bend: AF_B	30.3	1.03
Propagation: AF_P	33.1	1.13
Resistive Load: AF_R	34.1	1.17
End Reflection: AF_E	53.5	1.83

14. CONCLUDING COMMENTS

The results presented here were developed using the computer model TWTD [19] to estimate a quantitative relationship between an accelerated charge pulse on a PEC wire and the radiation that acceleration produces. The estimates developed for what is denoted here as an acceleration factor (AF) cannot be considered numerically precise. This is not because the TWTD results are uncertain, as TWTD has been extensively validated. It is instead because there is no clear-cut way for choosing at what time a reflected Qc pulse should be “measured” for comparison with the time variation of

its radiated E-field. This is true whether the pulse shapes themselves are used or when it is only their peak amplitudes are needed to estimate an AF . Thus, the AF values given throughout the text and summarized in Table 1, being derived from a computational “experiment”, must be considered as approximations. Also an issue in this respect is the fact that the actual acceleration depends on the specific nature of the physical feature that determines it. This is demonstrated, for example, in the values of AF_E and AF_S that might be expected to be in a ratio of 2 : 1 given their respective speed-change ratio of $2c/c$. The numerical value actually obtained is somewhat less at 1.83. In spite of the limitations involved, the numerical results obtained do provide a quantitative insight into the relative effects of various radiating features on a generic wire object and do demonstrate a consistent proportionality between the radiated E-field and the charge that produces it.

REFERENCES

1. Panofsky, W. K. H. and M. Phillips, *Classical Electricity and Magnetism*, Addison-Wesley Publishing Company, Inc., 1955.
2. Martin, R. G., A. R. Bretones, and S. G. Garzia, “Some thoughts about transient radiation by straight thin wires,” *IEEE Antennas and Propagation Society Magazine*, Vol. 41, No. 3, 24–33, 1999.
3. Bantin, C. C., “Radiation from a pulse-excited thin wire monopole,” *IEEE Antennas and Propagation Society Magazine*, Vol. 43, No. 3, 64–69, 2001.
4. Schelkunoff, S. A., *Advanced Antenna Theory*, 190, John Wiley & Sons, 1952.
5. Manneback, C., “Radiation from transmission lines,” *AIEE Journal*, Vol. 42, 95–105, Feb. 1923.
6. Jackson, J. D., *Classical Electrodynamics*, 401, John Wiley & Sons, 1962.
7. Yeh, Y. S. and K. K. Mei, “Theory of conical equiangular-spiral antennas Part II — Current distributions and input impedances,” *IEEE Trans. AP-S*, Vol. 16, No. 1, 14–21, 1968.
8. Shen, L.-C., T. T. Wu, and R. W. P. King, “A simple formula of current in dipole antennas,” *IEEE Trans. AP-S*, Vol. 16, No. 5, 542–547, 1968.
9. Bach Anderson, J., “Admittance of infinite and finite cylindrical metallic antenna,” *Radio Science*, Vol. 3, No. 6, 607–621, 1968.
10. Jones, D. S., *Methods in Electromagnetic Wave Propagation*, 295, Clarendon Press, 1994.
11. Kudrin, A. V., E. Yu. Petrov, G. A. Kyriacou, and T. M. Zaboronkova, “Insulated cylindrical antenna in a cold magnetoplasma,” *Progress In Electromagnetics Research*, Vol. 53, 135–166, 2005.
12. Jackson, J. D., “How an antenna launches its input power into radiation: The pattern of the Poynting vector at and near an antenna,” *Am. J. Phys.*, Vol. 74, 280–288, 2006.
13. Kordi, B., R. Moini, and V. A. Rakov, “Comment on ‘Return stroke transmission line model for stroke speed near and equal that of light’ by R. Thottappillil, J. Schoene, and M. A. Uman,” *Geophys. Res. Lett.*, Vol. 29, No. 10, 1369, 2002.
14. Kordi, B., R. Moini, and V. A. Rakov, “Comparison of lightning return stroke electric fields predicted by the transmission line and antenna theory models,” *Proc. 15th Int. Zurich Symp. Electromagn. Compat.*, 551–556, 102P2, Zurich, 2003.
15. Baba, Y. and M. Ishii, “Characteristics of electromagnetic return-stroke models,” *IEEE Trans. Electromagn. Compat.*, Vol. 45, No. 1, 129–135, Feb. 2003.
16. Baba, Y. and V. A. Rakov, “On the mechanism of attenuation of current waves propagating along a vertical perfectly conducting wire above ground: Application to lightning,” *IEEE Transactions of Electromagnetic Compatibility*, Vol. 47, No. 3, Aug. 2005.
17. Miller, E. K., “The differentiated on-surface poynting vector as a measure of radiation loss from wires,” *IEEE Antennas and Propagation Society Magazine*, Vol. 48, No. 6, 21–32, Dec. 2006.
18. Smith, G. S., *An Introduction to Classical Electromagnetic Radiation*, Cambridge University Press, 1997.

19. Landt, J. A., E. K. Miller, and M. Van Blaricum, "WT-MBA/LLL1B (TWTD): A computer program for the time-domain electromagnetic response of thin-wire structures," Lawrence Livermore Laboratory Report No. UCRL-51585, 1974.
20. Burke, G. J., E. K. Miller, and A. J. Poggio, "The numerical electromagnetics code (NEC) — A brief history," *2004 IEEE Int. Antennas Propagat. Symp. Dig.*, Vol. 42, 2871–2874, 2004.
21. Miller, E. K. and G. J. Burke, "A multi-perspective examination of the physics of electromagnetic radiation," *Applied Computational Electromagnetics Society Journal*, Vol. 16, No. 3, 190–201, 2001.
22. Miller, E. K., "Time-domain far-field analysis of radiation sources," *IEEE Antennas and Propagation Society Magazine*, Vol. 53, No. 5, 46–54, Oct. 2011.
23. Balanis, C., *Antenna Theory Analysis and Design*, Harper and Rowe Publishers, 1082.
24. Miller, E. K. and J. A. Landt, "Direct time-domain techniques for transient radiation and scattering from wires," *Proc. IEEE*, Vol. 68, 1396–1423, 1980.